

Doping-driven pseudogap-metal-to-metal transition in correlated electron systems

L. Fratino¹, S. Bag¹, A. Camjayi², M. Civelli¹, M. Rozenberg¹

¹ *Université Paris-Saclay, CNRS Laboratoire de Physique des Solides, 91405, Orsay, France*

² *Departamento de Física, FCEyN, UBA and IFIBA, Conicet, Pabellón 1, Ciudad Universitaria, Buenos Aires 1428 CABA, Argentina*

(Dated: January 20, 2022)

We establish that a doping-driven first-order metal-to-metal transition, from a pseudogap metal to Fermi Liquid, can occur in correlated quantum materials. Our result is based on the exact Dynamical Mean Field Theory solution of the Dimer Hubbard Model. This transition elucidates the origin of many exotic features in doped Mott materials, like the pseudogap in cuprates, incoherent bad metals, enhanced compressibility and orbital selective Mott transition. This phenomenon is suggestive to be at the roots of the many exotic phases appearing in the phase diagram of correlated materials.

Electronic correlations put into question our current understanding of metals. Emblematic is the case of Mott insulators¹⁻³ (like e.g. transition metal oxides, Bechgaard organic salts, alkali-doped fullerenes, twisted bilayer graphene, etc). According to the standard Bloch band-theory, these materials should be metals, but they turn out to be robust insulators because of dominating electronic correlations^{4,5}. Upon doping, a metallic state is recovered, but often displaying unconventional properties. One of the most striking examples is the so called pseudogap (PG) metal^{6,7} that appears for small doping in the phase diagram of cuprates superconductors, and which remains still poorly understood⁸. A conventional metallic phase, which can be described within the conventional Fermi Liquid (FL) Theory, is reestablished only for high doping⁹.

How the correlated Mott insulator evolves through those “bad metallic” states into the FL as a function of doping has remained a key open issue, not only in the context of cuprates. A point of view, that can be ascribed to the early work of P.W. Anderson⁴, advocates the existence of a new kind of metallic state, characterized by the absence of any broken symmetry even at the lowest temperatures. In this state, carriers have to move through a background described as a liquid of dynamical singlets, the RVB state. Another point of view advocates the existence of a quantum phase transition between an exotic order-parameter metal and the conventional FL^{10,11}. Unconventional phenomena, like the PG in cuprates, would then be the byproduct of this order parameter. In most cases, however, it has been difficult or impossible to identify such order, and the issue has remained openly debated (see e.g. the aforementioned PG phase or the so called hidden order in URu₂Si₂^{12,13}). Recent proposals have attempted to reconcile these two scenarios by introducing the concept of inter-twinning^{14,15}, or competition^{16,17} of different orders to form a new un-ordered unconventional phase, akin to Anderson’s proposal⁴. Establishing the existence of the PG-metal-to-metal transition is therefore a fundamental step within this open debate that could allow us to finally unveil the origin of key phenomena in correlated electron physics, like the high temperature superconductivity.

Recent works¹⁸⁻²⁴, within the context of the two-

dimensional Hubbard-like Models studied with state of the art methods like cluster extensions of the Dynamical Mean Field Theory (DMFT) have proposed the existence of a first order quantum phase transition between a PG and a FL metals as a function of doping. In two dimensions, however, only approximate solutions can be provided. Unfortunately, issues such as the “minus sign problem” prevent those state-of-the-art methods to obtain complete phase diagrams as a function of interaction, chemical potential and temperature²⁵. A consensus on the existence of the metal-to-metal transition has not been achieved yet.

Here we provide a concrete answer to this problem by an exact DMFT solution of a minimal model Hamiltonian, which establishes the existence of the first-order PG metal to FL metal transition. We focus on the dimer Hubbard Model (DHM), which a priori has the necessary ingredients to capture the relevant physics, namely, strong local Coulomb repulsion and non-local magnetic exchange interactions. The latter is a key feature, which is missing in the single-site Hubbard model, but is present in the 2D models mentioned before. However, in contrast to the 2D models, the DHM has the significant merit that it can be exactly solved within DMFT^{26,27}. Our results partially reconcile the debate between PG-metal vs quantum phase transition scenarios. We find that upon doping the DHM Mott state, an unconventional bad metal appears, displaying PG features reminiscent of the PG in cuprates and possessing a dominant spin-singlet component, akin to Anderson’s proposal⁴. Differently from the latter, however, a first order quantum phase transition to a more conventional FL does take place by further increase of doping. This PG-metal-to-metal transition, however, does not need to advocate for an elusive order parameter, but appears to be of the liquid-vapor type¹⁸⁻²¹.

Similarly to the case of the Mott metal-insulator transition in the single site Hubbard model, our present results suggest that the PG-metal-to-metal transition in the DHM may have universal character within correlated quantum materials. As we shall see, many unconventional properties of correlated materials are naturally realized in the solution of the model, such as a pseudogap, incoherent or bad metallicity, enhanced compressibility,

and orbital selectivity. Thus, we may argue that the present PG-metal-to-metal transition may be the long-sought phenomenon where many exotic quantum states find their roots¹⁵.

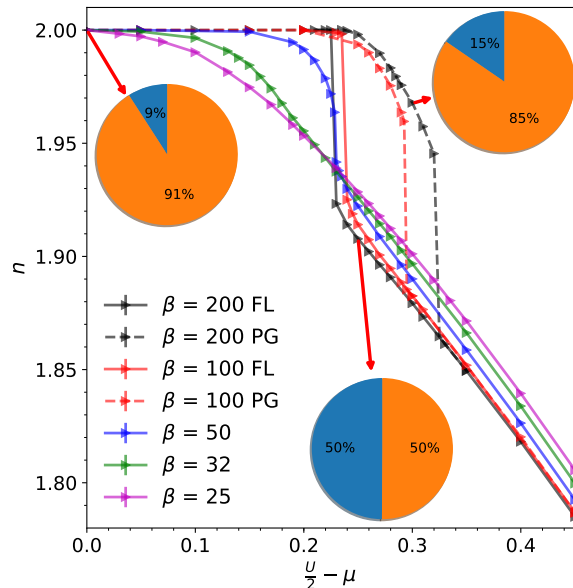


Figure 1. The electron density n as function of the renormalized chemical potential $\frac{U}{2} - \mu$. Half-filling corresponds to $n = 2$, where the system is a Mott insulator. The hysteresis behavior below $\beta = 50$ defines a PG-metal-to-metal coexistence region. Note the enhancement of the compressibility at the endpoint of the first order transition (blue line) at $\beta = 50$. The orange sector of the pie-charts indicates the relative contribution of the singlet states to the DAIM wavefunction projected on the isolated dimer. The blue sector corresponds to all other states (see details in the SM²⁸).

The Dimer Hubbard Model (DHM) consists of a lattice of dimers:

$$\mathcal{H} = \sum_{i,j;\sigma=\uparrow,\downarrow} \psi_{i,\sigma}^\dagger \mathbf{T}_{i,j} \psi_{j,\sigma} + U \sum_{i;\alpha=1,2} n_{i\alpha\uparrow} n_{i\alpha\downarrow} \quad (1)$$

The spinor $\psi_{i,\sigma} = (c_{i,1,\sigma}, c_{i,2,\sigma})$ acts on the dimer sites $\alpha = 1, 2$ at the lattice site i , being $c_{i\alpha\sigma}^\dagger, c_{i\alpha\sigma}$ the electron creation and destruction operators respectively. The matrix $\mathbf{T}_{i,j} = -t\hat{1}$ and $\mathbf{T}_{i,i} = -\mu\hat{1} + t_\perp\hat{\sigma}_x$ ($\hat{\sigma}_x$ is the first Pauli matrix) describes the nearest-neighbor inter-dimer and the intra-dimer electron hopping respectively. Electrons experience strong correlation via the on-site local repulsion U . We adopt $t = 0.5$ and $t_\perp = -0.3$, and fix the on-site local repulsion term $U = 2.3$ in order to be deep in the correlated regime. The same set of parameters has previously been considered in the study of the model at half-filling, where it exhibits a first-order temperature-driven insulator-to-metal transition^{27,29}. Here, we shall also vary the chemical potential μ to induce a doping-driven insulator-to-metal transition by adding or removing electrons.

The advantage of the DHM is that in the infinite dimensional limit DMFT provides the exact solution^{26,27,29–33}. We can then establish properties of the doped metallic state and its possible phase transitions without the uncertainty introduced by an approximation, such as in the CDMFT treatments of the 2D Hubbard model on a square lattice. It is convenient to express the DMFT equations in the diagonal bonding/anti-bonding (B/AB) basis of the lattice hopping matrix $\mathbf{T}_{i,j}$. The dimer Green's function in the B/AB basis can be written in terms of the components of site basis Green's function $G_{\alpha\beta}$ as $\text{diag}(G_B, G_{AB}) = \text{diag}(G_{11} - G_{12}, G_{11} + G_{12})$, where we dropped the spin indices for clarity. In the infinite dimensional limit, adopting a semicircular (i.e. Bethe lattice) density of states $D(\epsilon) = -\frac{1}{t\pi} \sqrt{(1 - (\frac{\epsilon}{2t})^2)}$, the DMFT self-consistency equations are then readily written:

$$\mathcal{G}_{oB/AB}^{-1}(\omega) = \omega + \mu \pm t_\perp - t^2 G_{B/AB}(\omega) \quad (2)$$

where $\mathcal{G}_{oB/AB}(\omega)$ is the Weiss field describing the bath of the dimer Anderson impurity model (DAIM) associated to the Hamiltonian (1). We solve the DAIM imaginary-time action

$$S_{\text{DAIM}} = - \int_0^\beta d\tau d\tau' \sum_{\substack{\sigma=\uparrow,\downarrow \\ \alpha,\beta=1,2}} c_{\alpha\sigma}^\dagger(\tau) \mathcal{G}_{o\alpha\sigma,\beta\sigma}^{-1}(\tau - \tau') c_{\beta\sigma}(\tau') + U \int_0^\beta d\tau \sum_{\alpha=1,2} n_{\alpha\uparrow}(\tau) n_{\alpha\downarrow}(\tau) \quad (3)$$

using the Continuous Time QMC (CTQMC) within the Hybridization Expansion approach^{34,35}. The self-consistent determination of Eq.s (2) and (3) outputs $G_{B/AB}(\omega)$ and the respective self-energies, which embody all the physical information that we need.

Our main result is shown in Fig.1, where we display the total density n as a function of the chemical potential $U/2 - \mu$, shifted with respect to the half-filled case. As previously reported^{27,29}, for $\mu = U/2$ the system is in a Mott insulator. This can be right away seen by following the n vs. $U - \mu/2$ behavior at the lowest temperatures T . It displays the horizontal plateau of electronic incompressibility at half-filling $n = 2$, which is the hallmark of a Mott insulating state. By varying μ , we can dope particles and holes so to drive a transition to a metallic state. Here we consider the hole-doping case, i.e. $n < 2$ (note that data would be symmetric for particle doping). At high temperatures ($T = 1/\beta > 1/20$), the transition to a metal takes place at small chemical potential $U/2 - \mu$, due to the fact that the thermal excited states occupying the Mott gap are available for adding holes. At smaller temperatures, the metallic state emerges more steeply at the plateau edge. For $\beta = 50$, we can observe that around $U/2 - \mu \simeq 0.21$, the system is already deep in the metallic state and the slope of the n vs $U/2 - \mu$ curve is markedly steep. This marks a diverging charge compressibility ($\propto dn/d\mu$) which is a typical signature of the onset

of a phase transition³⁶ (see SM²⁸ for more details). Indeed, by further reducing temperature ($T = 1/\beta < 1/50$) a coexistence region between two distinct metallic solutions, one coming from the insulator, which we shall show is a PG metal, and the other a FL coming from high doping, emerges and signals a first order metal-to-metal transition.

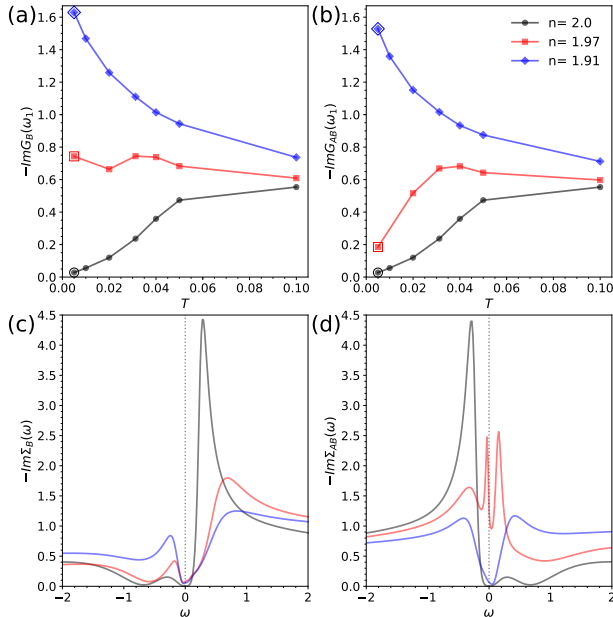


Figure 2. Panels (a) and (b): Respectively, $-\text{Im}G_B(\omega_1)$ and $-\text{Im}G_{AB}(\omega_1)$ as a function of T for densities $n = 2.0, 1.97, 1.91$, where ω_1 is the first Matsubara frequency. Panels (c) and (d): Respectively, $-\text{Im}\Sigma_B(\omega)$ and $-\text{Im}\Sigma_{AB}(\omega)$ as a function of real frequency ω for the same densities and the lowest temperature $T = 1/\beta = 0.005$.

To gain insight into the nature of these two qualitatively different metallic phases, we display in Fig. 2a,b the imaginary part of the dimer Green's function, $G_{B/AB}(\omega_1)$, which directly outputs from the CTQMC-DMFT, evaluated at the first Matsubara frequency ω_1 , as a function of temperature. This is a useful quantity as it is a measure of the spectral intensity at low frequency. Moreover, for $T \rightarrow 0$ it approaches the $D(E_F)$, thus providing a convenient criterion to distinguish metal from insulator states. A conventional FL metal is characterized by the presence of a quasiparticle spectral weight at the Fermi level. Indeed, at doping $n = 1.91$ (blue-diamond line), we observe that both $\text{Im}G_{B/AB}(\omega_1)$ approach a similar finite value for $T \rightarrow 0$. The high doping phase is therefore a normal correlated FL. In contrast, in the insulating phase at half-filling $n = 2$, the low frequency spectral weight gets depleted ($\text{Im}G(\omega_1) \rightarrow 0$ as $T \rightarrow 0$) as the Mott gap opens.

The interesting behaviour appears for $n = 1.97$ in the low doping metallic phase. While the B contribution displays metallic behavior as $G_B(\omega_1)$ extrapolates to a finite

value for $T \rightarrow 0$, the AB contribution, in contrast, loses spectral intensity at low frequency. Indeed, $\text{Im}G_{AB}(\omega_1)$ extrapolates to 0, or to a small finite value, when $T \rightarrow 0$. This anomalous state is an instance of orbital selectivity, which we call the PG metal³⁷.

To better understand the physical meaning of these results, it is useful to display on the real-axis the imaginary part of the corresponding self-energy $\Sigma_{B/AB}(\omega) = \mathcal{G}_{oB/AB}^{-1}(\omega) - G_{B/AB}^{-1}(\omega)$. The analytical continuation to the real axis of the CTQMC was obtained with a standard maximum entropy method. The self-energies are a measure of the correlation contribution to the many-body system and reveal the qualitatively different nature of the metallic states (see Fig. 2c,d). We can first discuss the more conventional Mott-insulator and FL phases at $n = 2.0$ and $n = 1.91$, respectively. Similarly to the familiar case of the single-site Mott insulator, where the correlation gap opens due to a pole in $\Sigma(\omega = 0)$, in the DHM the Mott gap opens by the same mechanism. More specifically, as seen in Fig. 2c,d, the intra-dimer hopping splits the pole symmetrically in $\Sigma_{B/AB}$ at $\omega = \pm t_{\text{perp}}$, respectively^{27,29}. The behavior of the self-energies sheds additional light on the physics of the DHM Mott insulator state. In contrast to the single-site case, where the localized electrons are incoherent spin-1/2, here they are in dimers that form a liquid of singlets, as envisioned by Anderson⁴. Thus, the electrons spend most of their time within a well defined quantum state, which gives them a long-lived quasiparticle-like character, which is reflected in the behavior of $\text{Im}\Sigma \rightarrow 0$ at $\omega \rightarrow 0$.

Upon doping, the peak feature is strongly reduced, the Mott gap closes, and the relevant energy scale is close to $\omega = 0$. In a metal, the FL prescription requires that $\text{Im}\Sigma \sim \omega^2$. This behavior is observed in the FL phase ($n = 1.91$ blue line), both in the $\text{Im}\Sigma_{B/AB}$, in agreement with the behavior of $\text{Im}G_{AB}$ discussed in Fig. 2a,b. On the other hand, in the PG metal ($n = 1.97$ red line), while the $\text{Im}\Sigma_B$ still displays a FL behavior at low frequency, the $\text{Im}\Sigma_{AB}$ completely breaks the FL, displaying a peak-like behavior at $\omega = 0$, reminiscent of previous results on a slightly doped Mott-Hubbard insulator in 2D^{22,37}.

The PG-metal appears to be smoothly connected to the Mott insulating state, as shown by the smooth evolution of the plateau in n vs. μ seen in Fig. 1¹⁸. The origin of the PG insulating component can be traced back to the Mott insulating state, which in the DHM is sharply distinct from the paramagnetic Mott insulator of single-site DMFT^{27,29}. In the DHM the physical properties are dominated by singlet formation (via correlation enhancement of the intra-dimer hopping t_{\perp} ²⁷), which is a non-local magnetic interaction that competes with the on-site Kondo mechanism. To show this connection, in Fig. 1 we display pie charts showing the singlet contribution to the wave-function projection on the dimer sites. In the Mott insulator the singlet contribution is 91%, and it is still a largely majoritarian 85% in the PG phase, once holes are introduced into the systems. This must be contrasted with FL phase, where the singlet appear to have

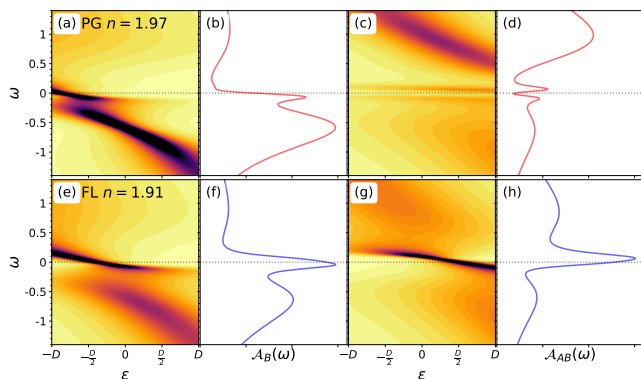


Figure 3. Electronic dispersion $A_{B/AB}(\omega, \epsilon)$ and local density of states $A_{B/AB}(\omega) = \int d\epsilon A_{B/AB}(\omega, \epsilon)$ (B first and second column and AB third and fourth). Top line has the PG-metal and the bottom line the FL-metal.

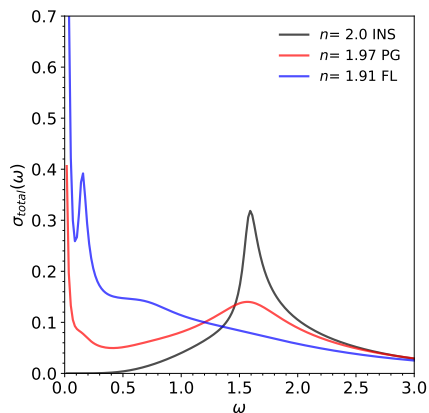


Figure 4. Optical conductivity in the insulating ($n = 2.0$) in black, PG ($n = 1.97$) in red and FL phases ($n = 1.91$) in blue.

a 50% contribution, comparable with that of other components (see SM²⁸ for details about this analysis). The PG phase can be qualitatively viewed as a soup of singlets and strongly damped (as described by $-\text{Im}\Sigma_B(\omega)$ in Fig.2c) FL-like hole carriers.

We argued before that the DHM PG-metal exhibits orbital selectivity. We shall now show that, interestingly, that state bears resemblance to the results from cluster extensions of the Hubbard Model in 2D^{38–40}, where the PG-state was argued to emerge from a “momentum-selective” Mott transition^{19,41–44}. This can be seen from the ϵ -resolved spectral functions $A(\omega, \epsilon)$, where single particle energy ϵ plays a similar role as the lattice momentum⁴⁵, since $A_{B/AB}(\omega, \epsilon) = \text{Im}[1/(\omega + \mu - \epsilon - \Sigma_{B/AB}(\omega))]$. The results are shown in Fig. 3, which we obtain by analytic continuation. At small doping ($n = 1.97$), we obtain the PG metal solution. In the B component, a coherent and dispersive narrow band ap-

pears at the Fermi level, which produces a narrow FL peak in the respective DOS. In stark contrast, the AB component develops two parallel and weakly-dispersive features around the Fermi level, which produce the PG-like dip in the DOS. Therefore, the PG metal possesses at the same time FL and non-FL character, qualitatively similar to the cluster extension and in strong analogy with the physics of cuprates. On the other hand, at higher doping ($n = 1.91$), the orbital selectivity disappears at low frequency. Both components display similarly dispersive coherent quasiparticle bands and quasiparticle peaks in the respective DOS, as expected in a conventional FL.

Finally, we obtained the optical conductivity that we show in Fig.4 for the Mott insulator along with the PG and the FL metal states²⁷. The Mott insulator has as expected a wide gap (black line $n = 2$). In contrast, at high doping (blue line $n = 1.94$) the optical response, as expected in a correlated metal with quasiparticles, has a narrow Drude peak at low frequency, whose spectral intensity denotes the effective carrier density. In addition, there is a mid-infrared contribution that has been previously identified as originated in the intra-dimer hopping²⁷. Interestingly, in between these two states we find the optical response of the PG-metal (red line $n = 1.97$), which combines features of both. At low frequency, it shows a narrow and relatively small Drude peak that can be traced to the FL-metal of the B component. This contribution coexists with significant mid-infrared intensity, which is featureless as it is associated to the incoherent PG state realized in the AB component. It is interesting to note that this optical conductivity response bears strong resemblance with the one observed in the PG phase of cuprates^{46,47}.

To conclude, we obtained the numerical quantum Monte Carlo solution on the Dimer Hubbard Model within DMFT, which is the exact solution of the model in the limit of large dimensions. This model is arguably the minimal Hubbard-like model that embodies on equal footing on-site correlations and non-local magnetic interactions. Our main result was to establish the existence of the doping-driven first order metal-to-metal transition between a pseudogap metal and a Fermi Liquid one. Moreover, the scenario that emerges from our findings help to clarify an important on-going debate. It provides a concrete realization and an explicit rational for the origin of several unconventional properties such as bad metal behavior, the pseudogap, orbital selective Mott transitions and enhanced compressibilities^{19,21,43,44,48}, which are relevant to doped Mott insulators and correlated quantum materials in general^{14,16,49}.

SB, MC and MR acknowledge support from the French ANR “MoMA” project ANR-19-CE30-0020. LF is supported by the UCSD-CNRS collaboration Quantum Materials for Energy Efficient Neuromorphic Computing, an Energy Frontier Research Center funded by the US Department of Energy, Office of Science, Basic Energy Sciences under award DE-SC0019273.

- ¹ N. F. Mott. *Rev. Mod. Phys.*, 40:677–683, 1968. URL <https://link.aps.org/doi/10.1103/RevModPhys.40.677>.
- ² Masatoshi Imada, Atsushi Fujimori, and Yoshinori Tokura. *Rev. Mod. Phys.*, 70:1039–1263, 1998. URL <https://link.aps.org/doi/10.1103/RevModPhys.70.1039>.
- ³ Philip Phillips. *Rev. Mod. Phys.*, 82(2):1719–1742, 2010. URL <https://journals.aps.org/rmp/abstract/10.1103/RevModPhys.82.1719>.
- ⁴ P. W. Anderson. *Science*, 235(4793):1196–1198, 1987. ISSN 0036-8075. URL <https://science.sciencemag.org/content/235/4793/1196>.
- ⁵ C.M. Varma, S. Schmitt-Rink, and Elihu Abrahams. *Solid state communications*, 62(10):681–685, 1987. URL <https://www.sciencedirect.com/science/article/abs/pii/0038109887904078>.
- ⁶ W.W. Warren Jr., R.E. Walstedt, G.F. Brennert, R.J. Cava, R. Tycko, R.F. Bell, and G. Dabbagh. *Physical review letters*, 62(10):1193, 1989. URL <https://journals.aps.org/prl/abstract/10.1103/PhysRevLett.62.1193>.
- ⁷ H. Alloul, T. Ohno, and P. Mendels. *Physical review letters*, 63(16):1700, 1989. URL <https://journals.aps.org/prl/abstract/10.1103/PhysRevLett.63.1700>.
- ⁸ Michael R. Norman, D. Pines, and C. Kallin. *Adv. Phys.*, 54:725, 2005.
- ⁹ D. C. Peets, J. D. F. Mottershead, B. Wu, I. S. Elfimov, Ruixing Liang, W. N. Hardy, D. A. Bonn, M. Raudsepp, N. J. C. Ingle, and A. Damascelli. *New Journal of Physics*, 9(2):28–28, 2007. URL <https://doi.org/10.1088/1367-2630/9/2/028>.
- ¹⁰ Subir Sachdev. *physica status solidi (b)*, 247(3):537–543, 2010. URL <https://onlinelibrary.wiley.com/doi/abs/10.1002/pssb.200983037>.
- ¹¹ Chandra M. Varma. *Reports on Progress in Physics*, 79(8):082501, 2016. URL <https://doi.org/10.1088/0034-4885/79/8/082501>.
- ¹² T. T. M. Palstra, A. A. Menovsky, J. van den Berg, A. J. Dirkmaat, P. H. Kes, G. J. Nieuwenhuys, and J. A. Mydosh. *Phys. Rev. Lett.*, 55:2727–2730, 1985. URL <https://link.aps.org/doi/10.1103/PhysRevLett.55.2727>.
- ¹³ J. A. Mydosh, P. M. Oppeneer, and P. S. Riseborough. *Journal of Physics: Condensed Matter*, 32(14):143002, 2020. URL <https://doi.org/10.1088/1361-648x/ab5eba>.
- ¹⁴ Eduardo Fradkin, Steven A. Kivelson, and John M. Tranquada. *Rev. Mod. Phys.*, 87:457–482, 2015. URL <https://link.aps.org/doi/10.1103/RevModPhys.87.457>.
- ¹⁵ B. Keimer, S. A. Kivelson, M. R. Norman, S. Uchida, and J. Zaanen. *Nature*, 518(7538):179–186, 2015. ISSN 1476-4687. doi:10.1038/nature14165. URL <https://doi.org/10.1038/nature14165>.
- ¹⁶ K. B. Efetov, H. Meier, and C. Pépin. *Nature Physics*, 9(7):442–446, 2013. ISSN 1745-2481. doi:10.1038/nphys2641. URL <https://doi.org/10.1038/nphys2641>.
- ¹⁷ Subir Sachdev and Rolando La Placa. *Phys. Rev. Lett.*, 111:027202, 2013. URL <https://link.aps.org/doi/10.1103/PhysRevLett.111.027202>.
- ¹⁸ G. Sordi, K. Haule, and A.-M. S. Tremblay. *Phys. Rev. Lett.*, 104:226402, 2010. URL <https://link.aps.org/doi/10.1103/PhysRevLett.104.226402>.
- ¹⁹ G. Sordi, K. Haule, and A.-M. S. Tremblay. *Phys. Rev. B*, 84:075161, 2011. URL <https://link.aps.org/doi/10.1103/PhysRevB.84.075161>.
- ²⁰ G. Sordi, P. Sémon, K. Haule, and A.-M. S. Tremblay. *Phys. Rev. Lett.*, 108:216401, 2012. URL <https://link.aps.org/doi/10.1103/PhysRevLett.108.216401>.
- ²¹ L. Fratino, P. Sémon, Giovanni Sordi, and A.-M. S. Tremblay. *Scientific reports*, 6(1):1–6, 2016. URL <https://www.nature.com/articles/srep22715>.
- ²² Helena Bragança, Shiro Sakai, M. C. O. Aguiar, and Marcello Civelli. *Phys. Rev. Lett.*, 120:067002, 2018. URL <https://link.aps.org/doi/10.1103/PhysRevLett.120.067002>.
- ²³ Peter Cha, Nils Wentzell, Olivier Parcollet, Antoine Georges, and Eun-Ah Kim. *Proceedings of the National Academy of Sciences*, 117(31):18341–18346, 2020. URL <https://www.pnas.org/content/117/31/18341>.
- ²⁴ Subir Sachdev, Harley D. Scammell, Mathias S. Scheurer, and Grigory Tarnopolsky. *Phys. Rev. B*, 99:054516, 2019. URL <https://link.aps.org/doi/10.1103/PhysRevB.99.054516>.
- ²⁵ Thomas Schäfer, Nils Wentzell, Fedor Šimkovic, Yuan-Yao He, Cornelia Hille, Marcel Klett, Christian J. Eckhardt, Behnam Arzhang, Viktor Harkov, François-Marie Le Régent, Alfred Kirsch, Yan Wang, Aaram J. Kim, Evgeny Kozik, Evgeny A. Stepanov, Anna Kauch, Sabine Andergassen, Philipp Hansmann, Daniel Rohe, Yuri M. Vilck, James P. F. LeBlanc, Shiwei Zhang, A.-M. S. Tremblay, Michel Ferrero, Olivier Parcollet, and Antoine Georges. *Phys. Rev. X*, 11:011058, 2021. URL <https://link.aps.org/doi/10.1103/PhysRevX.11.011058>.
- ²⁶ .
- ²⁷ O. Nájera, M. Civelli, V. Dobrosavljević, and M. J. Rozenberg. *Phys. Rev. B*, 95:035113, 2017. URL <https://link.aps.org/doi/10.1103/PhysRevB.95.035113>.
- ²⁸ Supplemental Material available at <https://xxx.xxx.xxx>.
- ²⁹ O. Nájera, M. Civelli, V. Dobrosavljević, and M. J. Rozenberg. *Phys. Rev. B*, 97:045108, 2018. URL <https://link.aps.org/doi/10.1103/PhysRevB.97.045108>.
- ³⁰ Antoine Georges. *arXiv preprint cond-mat/0403123*, 2004. URL <https://arxiv.org/abs/cond-mat/0403123>.
- ³¹ Andreas Fuhrmann, David Heilmann, and Hartmut Monien. *Phys. Rev. B*, 73:245118, 2006. URL <https://link.aps.org/doi/10.1103/PhysRevB.73.245118>.
- ³² S. S. Kancharla and S. Okamoto. *Phys. Rev. B*, 75:193103, 2007. URL <https://link.aps.org/doi/10.1103/PhysRevB.75.193103>.
- ³³ H. Hafermann, M.I. Katsnelson, and A.I. Lichtenstein. *EPL (Europhysics Letters)*, 85(3):37006, 2009. URL <https://iopscience.iop.org/article/10.1209/0295-5075/85/37006/meta>.
- ³⁴ Emanuel Gull, Andrew J. Millis, Alexander I. Lichtenstein, Alexey N. Rubtsov, Matthias Troyer, and Philipp Werner. *Rev. Mod. Phys.*, 83:349–404, 2011. URL <https://link.aps.org/doi/10.1103/RevModPhys.83.349>.
- ³⁵ .
- ³⁶ .
- ³⁷ Michel Ferrero, Pablo S. Cornaglia, Lorenzo De Leo, Olivier Parcollet, Gabriel Kotliar, and Antoine Georges. *Phys. Rev. B*, 80:064501, Aug 2009. URL <https://link.aps.org/doi/10.1103/PhysRevB.80.064501>.
- ³⁸ B. Kyung, S. S. Kancharla, D. Sénéchal, A.-M. S. Trem-

- blay, M. Civelli, and G. Kotliar. *Phys. Rev. B*, 73:165114, 2006. URL <https://link.aps.org/doi/10.1103/PhysRevB.73.165114>.
- ³⁹ M. Civelli, M. Capone, S. S. Kancharla, O. Parcollet, and G. Kotliar. *Phys. Rev. Lett.*, 95:106402, 2005. URL <https://link.aps.org/doi/10.1103/PhysRevLett.95.106402>.
- ⁴⁰ Alexandru Macridin, M. Jarrell, Thomas Maier, P. R. C. Kent, and Eduardo D’Azevedo. *Phys. Rev. Lett.*, 97:036401, 2006. URL <https://link.aps.org/doi/10.1103/PhysRevLett.97.036401>.
- ⁴¹ Michel Ferrero, Pablo S. Cornaglia, Lorenzo De Leo, Olivier Parcollet, Gabriel Kotliar, and Antoine Georges. *Phys. Rev. B*, 80:064501, 2009. URL <https://link.aps.org/doi/10.1103/PhysRevB.80.064501>.
- ⁴² Emanuel Gull, Olivier Parcollet, Philipp Werner, and Andrew J. Millis. *Phys. Rev. B*, 80:245102, 2009. URL <https://link.aps.org/doi/10.1103/PhysRevB.80.245102>.
- ⁴³ G. Sordi, P. Sémon, K. Haule, and A.-M. S. Tremblay. *Phys. Rev. B*, 87:041101, 2013. URL <http://link.aps.org/doi/10.1103/PhysRevB.87.041101>.
- ⁴⁴ G Sordi, P Sémon, K Haule, and A-M S Tremblay. *Sci. Rep.*, 2, 2012. URL <http://www.nature.com/articles/srep00547>.
- ⁴⁵ Antoine Georges, Gabriel Kotliar, Werner Krauth, and Marcelo J. Rozenberg. *Rev. Mod. Phys.*, 68:13–125, 1996. URL <http://link.aps.org/doi/10.1103/RevModPhys.68.13>.
- ⁴⁶ D. N. Basov and T. Timusk. *Rev. Mod. Phys.*, 77:721–779, Aug 2005. URL <https://link.aps.org/doi/10.1103/RevModPhys.77.721>.
- ⁴⁷ S. L. Cooper, D. Reznik, A. Kotz, M. A. Karlow, R. Liu, M. V. Klein, W. C. Lee, J. Giapintzakis, D. M. Ginsberg, B. W. Veal, and A. P. Paulikas. *Phys. Rev. B*, 47:8233–8248, Apr 1993. URL <https://link.aps.org/doi/10.1103/PhysRevB.47.8233>.
- ⁴⁸ L. Fratino, P. Sémon, G. Sordi, and A.-M. S. Tremblay. *Phys. Rev. B*, 93:245147, 2016. URL <http://link.aps.org/doi/10.1103/PhysRevB.93.245147>.
- ⁴⁹ V. J. Emery, S. A. Kivelson, and H. Q. Lin. *Phys. Rev. Lett.*, 64:475–478, 1990. URL <https://link.aps.org/doi/10.1103/PhysRevLett.64.475>.